Journal of Organometallic Chemistry, 341 (1988) 495–509
Elsevier Sequoia S.A., Lausanne – Printed in The Netherlands

Halocarbon chelation in $[Ir(cod)(\eta^2\text{-}o\text{-}HalC_6H_4PPh_2)]SbF_6$ (Hal = Br, Cl): structural and chemical studies *

Mark J. Burk, Robert H. Crabtree

Chemistry Department, Yale University, 225 Prospect Street, New Haven, CT 06511 (U.S.A.)

and Elizabeth M. Holt

Chemistry Department, Oklahoma State University, Stillwater, O.K. 74078 (U.S.A.)

(Received June 30th, 1987)

Abstract

The bromo- and chloro-arene groups of $Ph_2P(o\text{-}HalC_6H_4)$ (L^{Cl}, X = Cl; L^{Br}, X = Br) are nonchelating in [IrCl(cod)L] (**1**) but chelate to the metal in $[Ir(cod)L]SbF_6$ (**2**), as shown by ^1H and ^{31}P NMR and X-ray structural studies of both the L^{Cl} and L^{Br} species. The Ir–Hal distances of 2.381(4) and 2.473(4) Å, respectively, are normal covalent distances. The L^F analog of **1** is formed but an analog of **2** could not be made. **2** reacts with Cl^- to open the chelate ring to give **1** back again. MeCN adds to give a 5-coordinate species at −80 °C but this opens to the substitution product $[Ir(cod)(MeCN)(\eta^1\text{-}L^{Br})]SbF_6$ at room temperature. H_2 adds to give a dihydride, which is an alkene hydrogenation catalyst, even though **2** does not oxidatively add a C–Hal bond of the L ligand. C–Hal oxidative addition is presumed to be involved in the conversion of **2** to $[IrBr(cod)PPh_3)]$ by $LiBEt_3H$ or NaOCHO. LiMe give $[IrMe(cod)(\eta^1\text{-}L^{Br})]$. Selected crystal data (the data for the L^{Br} analogue is given first) are: *a* 13.127(1), 13.094(6); *b* 10.293(4), 10.184(4); *c* 12.007(8), 11.933(7) Å; α 68.12(4)°, 68.47(4)°; β 77.07(4)°, 76.75(4)°; γ 104.16(2)°, 103.59(3)°, $R = 9.6$, 6.7%. There is disorder in the SbF_6 and cod groups. Both species crystallize in the $P\bar{1}$ space group with $Z = 2$.

Halocarbon complexes of the type LnM ← X–R (X = halogen; R = alkyl, aryl) in which the C–X bond is intact have been proposed on several occasions [1] notably by Beck [2]. The failure of an X-ray structural study [3] to confirm the earliest proposal for such binding emphasizes the desirability of structural data in this area. We were able to obtain structural support for the iodocarbon complexation in $[IrH_2(o\text{-}C_6H_4I_2)(PPh_3)_2]^+$ [4a] and $[IrH_2(IMe)_2(PPh_3)_2]^+$ [4b], and have reported

* Dedicated to Prof. Colin Eaborn in recognition of his many contributions to chemistry.

preliminary structural data for the bromocarbon complex $[Ir(cod)\{o\text{-}C_6H_4X(PPh_2)\}]^+$ (X = Br) [4c]. We now report the full data on this and the chlorocarbon analog, together with some reactions of these species.

Other crystallographically-confirmed bromocarbon complexes have been observed more recently [5]. The X–M bond length for X = Cl, Br and I is appropriate for a single bond, but the M–F distances in the few known fluorocarbon adducts [6] are much longer than the sum of the covalent radii, and so 'secondary bonding' has been invoked in these cases.

We chose to study chelating phosphorus ligands in which a phosphorus atom brings the halocarbon into the close vicinity of the metal, because ^{31}P NMR is an excellent criterion [7] for distinguishing between chelation, cyclometallation (oxidative addition), and displacement of the halocarbon, and because the chemistry of phosphines is so well understood.

One of the key requirements for observing halocarbon complexes is that oxidative addition of the halocarbon to the metal does not occur. In the iridium(III) systems studied previously, this did not happen because $Ir^{III} \rightarrow Ir^{V}$ is usually an unfavorable transformation. It was therefore possible that halocarbon binding would prove to be a property only of high oxidation state complexes. We therefore chose iridium(I) for our next series of experiments both in order to check the generality of halocarbon binding and to see under what conditions cyclometalation (oxidative addition) would be observed.

Results and discussion

$[IrCl(cod)]$ reacts with $o\text{-}C_6H_4Br(PPh_2)$ $(= L^{Br})$ to give $[IrCl(cod)L^{Br}]$ (**1**) a yellow monomeric material closely resembling the PPh_3 analog. This compound could in principle contain 16e Ir^{I} and monodentate L^{Br} or 18e Ir^{I} and bidentate L^{Br}, or even 18e Ir^{III} and cyclometallated L^{Br}. It would be tedious to have to do a crystal structure at each step of this study, so we developed two spectroscopic criteria to distinguish between the different possible types of binding.

In chelated systems the ^{31}P NMR resonance of L^{Br} lies in the range δ +45 to 60 ppm and in unchelated ones at δ +15 to 30 ppm. On the other hand, cyclometallated $(o\text{-}C_6H_4PPh_2)$ groups resonate at ca. δ −20 to −35 ppm according to the

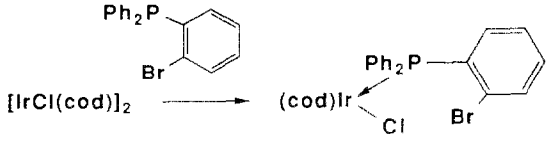

1

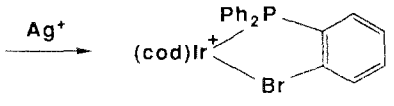

(1)

2

work of Garrou [7], who has documented the large and predictable changes in ^{31}P chemical shift with changes in the ring size of a phosphorus-containing molecule. In the case of 5-membered rings (i.e., L chelating via P and halogen), a shift of +25 to +33 ppm is expected; we observe shifts of +28 to +33 ppm (see below).

The second spectroscopic criterion is the appearance in the ^1H NMR only in unchelated systems of a multiplet corresponding to one proton at δ 6.8 to 7.2 ppm. It is always clear of the other aromatic protons which resonate to low field of δ 7.2 (7.2–7.8 ppm). This unique proton is most probably *ortho* to the halogen on the substituted ring. The diamagnetic shift due to the electrons of the halogen substituent may well be much reduced on binding, presumably because these electrons are perturbed by binding to Ir.

These criteria show that L^{Br} in **1** is monodentate. This is not surprising, since $[IrCl(cod)(PPh_3)_2]$ readily dissociates PPh_3 to give the analogous PPh_3 complex [8]. Perhaps more surprising is the fact that the bromoarene in **1** shows no tendency to cyclometallate even after 16 h at 110 °C even though bromoarenes generally give rapid oxidative addition to iridium(I) complexes, such as Vaska's compound [9].

We next treated **1** in CH_2Cl_2 with $AgSbF_6$ to remove the Cl^- from the iridium to give a 14-electron species which would be much more likely to bind the halocarbon. As expected the product, **2**, contains a chelating L^{Br} group. The ^{31}P NMR shows a peak at δ +52.7 ppm with a chelate shift relative to **1** of +32 ppm. In the ^1H NMR, aromatic resonances are only observed in the range δ 7.55–8.0 ppm, but not to high field of δ 7.2 ppm, again consistent with chelation.

Finally, the cod-vinyl resonances appear at δ 5.65 (*trans* to P) and 3.55 ppm (*trans* to Br). We have found [10] in complexes of the [IrX(cod)L] type that the

Table 1

Crystal data for the complexes studied

Formula	$IrSbClPF_6C_{26}H_{26}$	$IrSbBrPF_6C_{26}H_{26}$
Mol. wt.	832.9	877.3
a	13.094(6) Å	13.127(1) Å
b	10.184(4)	10.239(4)
c	11.933(7)	12.007(8)
α	68.47(4)	68.12(4)
β	76.75(4)	77.07(4)
γ	103.59(3)	104.16(2)
V	1348.4(12) Å^3	1360.3(10) Å^3
$F(000)$	792	1292
μMo-K_α	61.34 cm^{-1}	83.8 cm^{-1}
λMo-K_α	0.71069A	0.71069A
D_{calc}	2.05 g cm^{-3}	2.14 g cm^{-3}
Z	2	2
Obs. refl.	3863	3213
R	6.7%	9.6%
Space group	$P\bar{1}$	$P\bar{1}$

Matrix for conversion to reduced cell (all angles > 90 °):

$$\begin{vmatrix} 1 & 0 & 0 \\ 0 & 1 & 0 \\ 0 & 0 & -1 \end{vmatrix}$$

Table 2

Selected bond distances and angles (°)

	[Ir(cod)(η^2-L^{Cl})]SbF_6	[Ir(cod)(η^2-L^{Br})]SbF_6
Ir–Cl(1)	2.381(4)	–
Ir–Br(1)	–	2.473(4)
Ir–P(1)	2.288(5)	2.288(10)
Ir–C(1)	2.22(2)	2.18(4)
Ir–C(2)	2.20(2)	2.222(5)
Ir–C(5)	2.16(2)	2.17(3)
Ir–C(6)	2.12(2)	2.15(3)
C(1)–C(2)	1.37(3)	1.35(6)
C(5)–C(6)	1.54(4)	1.67(7)
C(12)–Cl	1.74(2)	–
C(12)–Br	–	1.86(2)
C(12)–Cl–Ir	106.2(5)	–
C(12)–Br–Ir	–	102.2(9)

cod-vinyl resonances in the ^{1}H NMR are very sensitive to the nature of the *trans* ligand. The weaker *trans*-influencing ligands lead to the *trans*-Ir(C=C) group having a greater metallacyclopropane character.

Table 3

Selected Positional Parameters ($\times 10^4$)

Atom	[Ir(cod)(η^2-L^{Cl})]SbF_6			[Ir(cod)(η^2-L^{Br})]SbF_6		
	x	y	z	x	y	z
Ir	1722(1)	9944(1)	6196(1)	1737(1)	9995(2)	6170(1)
Cl	145(4)	8290(5)	8099(4)	–	–	–
Br	–	–	–	106(3)	8334(4)	8170(3)
Sb	2580(1)	1222(2)	−145(1)	2649(2)	1266(3)	−196(3)
P	2137(3)	7816(5)	6447(4)	2114(6)	7852(9)	6442(8)
F(1)	1673(18)	2150(27)	−730(16)	1653(39)	1913(22)	−760(34)
F(2)	1461(18)	−115(18)	1417(17)	1475(33)	−166(26)	1286(34)
F(3)	3531(24)	446(42)	369(24)	3565(51)	445(96)	260(38)
F(4)	3664(20)	2611(24)	−1771(18)	3817(40)	2759(37)	−1730(44)
F(5)	2925(18)	2575(24)	507(19)	2953(35)	2341(35)	531(36)
F(6)	2180(21)	−66(24)	−822(23)	2343(39)	179(67)	−941(43)
C(1)	1645(16)	12045(19)	6320(16)	1705(29)	12069(32)	6267(32)
C(2)	915(16)	11644(22)	5747(17)	983(30)	11756(47)	5677(35)
C(3)	1108(22)	12387(27)	4337(22)	1147(38)	12461(60)	4251(36)
C(4)	2183(21)	12367(28)	3498(19)	2247(39)	11446(50)	3466(36)
C(5)	2608(17)	11241(25)	4154(16)	2591(35)	11326(55)	4117(32)
C(6)	3355(15)	11495(22)	4941(23)	3427(32)	11485(37)	4963(41)
C(7)	3698(19)	12774(28)	5185(27)	3774(34)	12779(48)	5152(46)
C(8)	2754(18)	13297(23)	5638(21)	2860(33)	13371(43)	5569(39)
C(11)	864(13)	6202(18)	7567(15)	849(24)	6207(35)	7556(27)
C(12)	5(13)	6474(19)	8292(15)	−21(25)	6418(39)	8316(30)
C(13)	−1012(14)	5298(23)	9152(16)	−1019(26)	5214(45)	9194(33)
C(14)	−1147(16)	3868(22)	9315(18)	−1145(28)	3776(44)	9298(33)
C(15)	−0311(16)	3527(21)	8653(19)	−293(31)	3466(41)	8595(34)
C(16)	862(15)	4740(21)	7785(17)	708(28)	4777(41)	7730(55)

We crystallized a sample of **2** and the X-ray structure (Tables 1–3) showed that the chelating structure is retained in the solid state. Disorder of the F atoms in the SbF_6 group and in C(4)-C(5) of the cod ligand lessened the quality of the structure; the final *R* factor was 9.6%. Fortunately the point at issue, namely the existence of an Ir–Br bond is unequivocally established. The bond length 2.473(4) Å is appropriate for a full covalent bond between Ir and Br and so, as in the case of the iodoarene complexes we studied previously [4a,4c], the halocarbon is fully coordinated and not simply involved in outer sphere or secondary interactions with the metal. This distance is considerably shorter than in the Foces-Foces compound [5a] (Rh–Br 2.660(1) Å) but similar to the distance in the Cotton and Lahuerta [5b] compound $IrCl_3(o\text{-}BrC_6F_4PPh_2)(PPh_3)$ (Ir–Cl 2.479(2) Å). The structure also shows the expected square planar arrangement and the η^4-cod ligand. We defer a more detailed examination of the structure to a later section, where we will compare it with its $o\text{-}C_6H_4Cl(PPh_2)$ ($= L^{Cl}$) analog.

Chemistry of the halocarbon complex

We were interested to see whether the bound halocarbon in **2** could be displaced by various ligands L. This turns out to be relatively easy. NaCl displaces the halocarbon to give back **1**.

More interesting behavior was observed with MeCN, one equivalent of which was sufficient to open the chelate ring, to give **3a**. This was suggested by the shift of the ^{31}P NMR resonance to δ +19.56 ppm, a nonchelating position, and the appearance of a ^1H NMR resonance at δ 6.8–7.05 ppm. Attempted crystallization of the product with Et_2O, led to precipitation of the original chelated complex **2**. The ^1H NMR data for **3a** showed only one cod-vinyl resonance instead of the two expected, one C=C group being *trans* to P and the other to N. We wondered whether this fluxionality could arise through the formation of a 5-coordinate intermediate $[Ir(cod)(NCMe)(\eta^2\text{-}L^{Br})]^+$ (**3b**). NMR data shows that the addition of equivalent of MeCN to **2** at −80 °C does indeed give **3b**. Ring opening by loss of the bromoarene to give **3a** only occurs on raising the temperatuare. At 25 °C, **3a** appears to be the dominant species; no doubt the ring opening has a large entropic driving force.

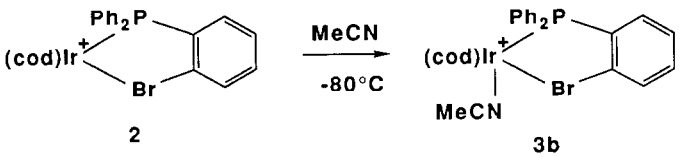

2 3b

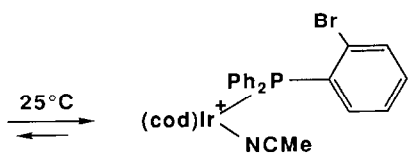

3a (2)

One important reason for this study was to understand how our alkane activation chemistry [11] (eq. 3) could proceed so well in halocarbon solvents:

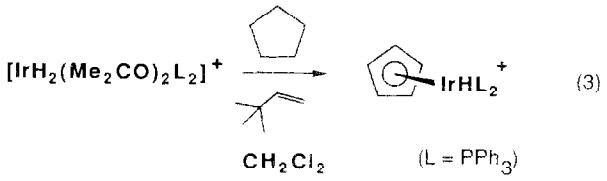

(3)

An iridium intermediate must react competitively with cyclopentane in the presence of halocarbon. This seems to require that oxidative addition to a C–H bond be kinetically favored over attack on a chlorocarbon C–H or C–Cl bond. The balance is close, however, and some C–Cl bond breaking does occur. Indeed, for the slightly less reactive alkane, cyclohexane, no alkane activation products are observed in halocarbon solvents, only C–Cl cleavage products [12]. Moving to alkane as solvent successfully dealt with this problem.

We therefore looked at the reaction of H_2 with **2** as a model for the oxidative addition of a C–H bond, which is important in the reaction sequence of eq. 3. We find that even at $-80\,^{\circ}C$ or at room temperature H_2 reacts to give the *cis*-dihydride **4** (eq. 4):

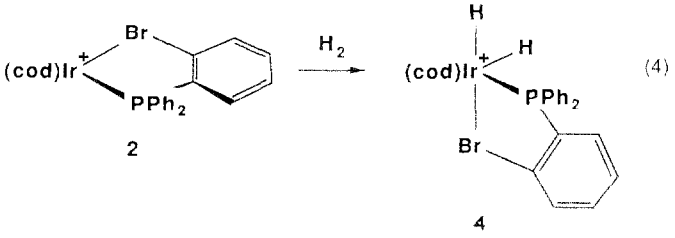

2 4

(4)

This shows that oxidative addition of H_2 does occur under conditions for which C–Br addition does not take place. It is not yet clear whether the reluctance of the C–Br bond to react is kinetic or thermodynamic. Arguments can be made for both possibilities. The mechanism of the reaction would be expected [13] to go by electron transfer from metal to halocarbon or by nucleophilic attack on the aromatic ring. Both require the metal *d*-electrons to be accessible. In fact, we have a system in which these electrons are less available, because of (i) the presence of the electron-withdrawing cod ligand, and (ii) the positive charge on the metal. Only the first factor is applicable in the case of **1**, which makes it difficult to judge how much each contributes. The addition of H_2 does not require the metal to be so electron rich as is the case for C–Br addition. A variety of cationic complexes, even ones containing very electron withdrawing ligands (e.g., $[(cod)_2Ir]^+$), readily add H_2 even at $-80\,^{\circ}C$ [10]. Saillard and Hoffman [14] have argued on theoretical grounds that $H_2 \rightarrow M$ charge transfer is important in the early stages of the oxidative addition of H_2. We and others [15–17] have isolated molecular hydrogen complexes and have suggested that $H_2(\sigma) \rightarrow M(d_\sigma)$ electron donation is the major factor involved in bond formation between the dihydrogen and the metal. Thermodynamic factors, particularly the strength of the M–H bonds to be formed, will then decide if the reaction will go on to oxidative addition or not.

Alternatively, thermodynamics may be involved in the failure of **1** and **2** to undergo oxidative addition of the C–Br group. Since the addition of H_2 to such cationic iridium species may have reducing character, this may give rise to a more stable product than the addition of a highly oxidizing C–Br bond. The latter would, for example, disfavor Ir(C=C) bonding by making the *d*-electrons even less available and this in turn might be enough to disfavor the addition. We hope to be able to answer this question of kinetics vs. thermodynamics by making a halocarbon oxidative addition adduct by an independent route and seeing if it loses halocarbon. This has not proved possible with this system.

Since **2** reacts with H_2 and can then go on the generate vacant sites by opening of the chelate ring, it seemed reasonable to try it as a hydrogenation catalyst. In CH_2Cl_2 under conditions in which [Ir(cod)(PCy_3)(py)]BF_4 (**5**) [17b] is active (1 atm H_2, 25 °C), 1-methylcyclohexene was reduced by **2** about 20 times slower than by **5**, but much faster than by $RhCl(PPh_3)_3$ in EtOH, which is very sluggish for trisubstituted olefins. The catalyst **2** was not active at 0 °C, however, because the dihydride **4** did not undergo H transfer to the cod ligand at that temperature; this step is of course necessary to obtain an active catalyst.

We tried to induce oxidative addition in a complex of L^{Br} by moving to a more electron-rich environment. The neutral complex [IrCl(cod)L^{Br}] (**1**) also failed to react after 6 h at 110 °C. In an attempt to make the hydride analog, we treated **2** with an equivalent of $LiBEt_3H$. The final product was [IrBr(cod)(PPh_3)] presumably formed by the sequence shown in Scheme 1. Since $Li[BEt_3H]$ is known to displace the halide from certain haloarenes to give the unsubstituted arene, we wondered whether this might be happening here. In order to distinguish between this route and the one shown in eq. 5 (Scheme 1), we needed a reducing agent sufficiently mild so that there was no question of nucleophilic attack of H^- at the ring. Sodium formate proved to be effective. We find that this reagent cleanly transfers H^- to $[(cod)IrL_2]^+$ by loss of CO_2 (eq. 6).

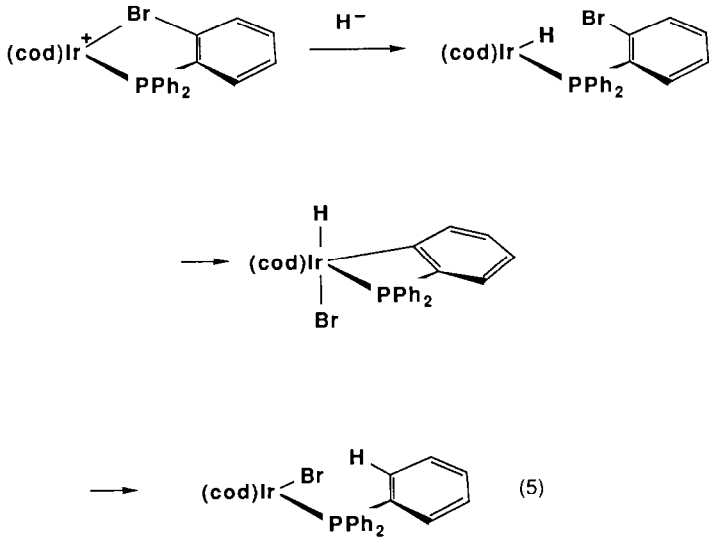

Scheme 1

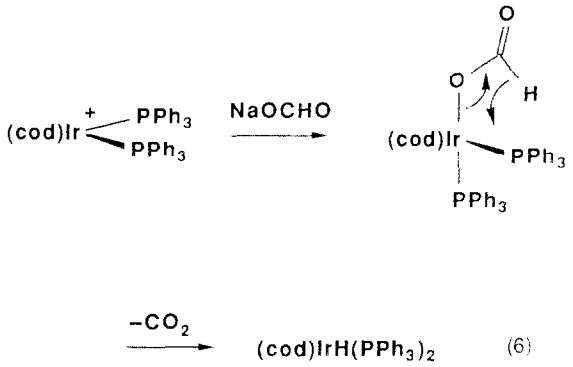

$$\xrightarrow{-CO_2} \quad (cod)IrH(PPh_3)_2 \qquad (6)$$

Reaction of sodium formate with **2** in CH_2Cl_2 over 36 h also gave [(cod)IrBr(PPh_3)] in 80% yield. In this case the reaction cannot occur by direct displacement of Br^- by attack of H^- on the ring and so we are left with the route of eq. 5 (Scheme 1).

In an effort to provide a deeper insight into the reaction we added MeLi to **2**. In this case an air-sensitive red methyl complex, [(cod)IrMe(η^1-L^{Br})] (**4**) was formed. The ^{31}P NMR resonance at +30.5 ppm shows that the ligand is unchelated. In the ^1H NMR, the methyl group appears as a doublet at δ 0.83 ppm (^3J(P,H) 6.2 Hz), and the presence of an absorption in the aromatic region (δ 6.6–6.75 ppm) confirms the nonchelating character.

No reaction takes place after heating the methyl complex **4** at 60 °C for 12 h in C_6D_6. At reflux, however, a reaction does take place. NMR evidence suggests that [(cod)IrBr(*o*-$MeC_6H_4PPh_2$)] may be the product (^1H NMR: cod-vinyl, δ 2.82 and 5.57 ppm; $MeC_6H_4PPh_2$, δ 3.22 ppm. ^{31}P NMR: δ +21.3 ppm) but we have not yet confirmed this by independent synthesis of the complex.

The addition of HBF_4 to the methyl complex **4** leads to the formation of **2** by loss of CH_4:

$$[IrMe(cod)(\eta^2\text{-}L^{Br})] + H^+ \rightarrow [Ir(cod)(\eta^2\text{-}L^{Br})]^+ + CH_4 \qquad (7)$$

Hydrogen addition at −80 °C can be followed by ^1H NMR spectroscopy in toluene-d_8. The dihydride shown in eq. 4 is formed. The peaks of this species then disappear with time and are replaced by those for CH_4 (δ 0.79 ppm) over 2 h at −80 °C. Ultimately, after warming to 25 °C, [(cod)IrBr(PPh_3)] is observed as product. The most reasonable pathway is reductive elimination of methane from the dihydride, followed by the oxidative addition/reduction elimination sequence of eq. 5. At −80 °C, an intermediate is observed by ^1H NMR with an Ir-*H* resonance at δ −12.1 ppm (^2J(P,H) 20 Hz). It is probably the cyclometallated intermediate or [(cod)IrH(η^1-LBr)], although solubility difficulties prevented us from looking at the ^{31}P NMR.

The same species [(cod)IrBr(PPh_3)] was observed from the reaction of $LiBEt_3H$ with [IrCl(cod)(η^1-L^{Br})] at −80 °C. We propose that [IrH(cod)(η^1-L^{Br})] is formed and that this reacts by the route of eq. 5.

The mechanism of C–Br oxidative addition

The isolation of these halocarbon complexes suggests a mechanism for oxidative addition in which the aryl group migrates directly from the halogen atom to the metal. Hoffmann et al. [18] have examined this possibility theoretically for the case of MeI and find it to be a reasonable pathway. A migration of this sort may also be involved in the cleavage of S–C and P–C bonds in SR_2 and PR_3 complexes, the latter being important in the deactivation of phosphine-containing homogeneous catalysts [19]:

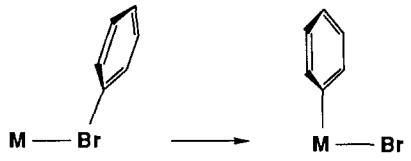

(8)

The chloroarene analogue

The analogous ligand *o*-$C_6H_4Cl(PPh_2)$ (= L^{Cl}) gave very similar chemistry to the bromocarbon analog. Both **5** and **6**, analogs of **1** and **2** were made in an analogous way. The ^{31}P NMR showed that **5** was nonchelating (δ +17.31 ppm) and **6** chelating (δ +45.9 ppm); the chelation shift is +28.6 ppm.

We were particularly interested in the structure, in order to make a more detailed comparison between the two ligands. The data (Tables 1–3, Fig. 1) show that the two analogues are almost isostructural. The Ir–Cl bond length is 2.381(4) Å, close to

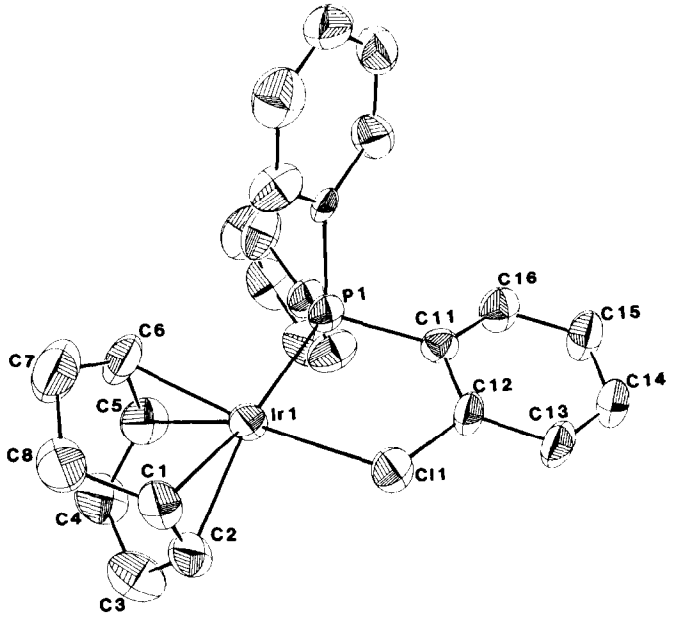

Fig. 1. The ORTEP diagram of the cation of the chelate complex [Ir(cod)(η^2-*o*-$ClC_6H_4PPh_2$)]SbF_6. The *o*-$BrC_6H_4PPh_2$ complex has an almost identical structure (for ORTEP diagram see ref. 4c).

the sum of the covalent radii, showing that the halocarbon is coordinated to the metal. This appears to be the first crystallographically-authenticated chlorocarbon complex.

A slight difference between the two structures is the C(12)–Cl–Ir angle of 106.2(5)° compared with C(12)–Br–Ir of 102.2(9)°. This can be compared somewhat less directly, it is true, with C–I–Ir of 100.9° (av.) and 106.8° (av.), in the structures of $[IrH_2(o\text{-}C_6H_4I_2)L_2]^+$ [4a] and $[IrH_2(MeI)_2L_2]^+$ [4c]. The Foces-Foces compound [5a] has a Rh–Br–C angle of 97.6(3)°, and the Cotton and Lahuerta [5b] compound an Ir–Br–C angle of 100.4°(5), even smaller than we see here. These angles are not dictated by the chelating character of the ligand. Two lines of evidence suggest this; the chelating and nonchelating iodocarbons have very similar angles, and the *ortho* substituted aromatic ring is bent out of the square plane of the 4-coordinate complexes and out of the equatorial plane of the 6-coordinate complexes. This bending reduces the value of the C–Hal–M angle from what it would be if the aryl group were in the plane of the complex.

The reason for the decrease in the C–Hal–M angle in the order Cl > Br > I probably comes about as a result of differing hybridization in the three systems. The lone pairs on RHal can be considered [19] to lie between the extreme representations of (i) a more stable *sp* hybrid and two *p*-orbitals at higher energy and (ii) three equivalent sp^3 orbitals. The greater shielding for the heavier elements will tend to separate the *s* and *p* levels and so favor model i for Cl and Br, but especially for I. Of the two types of lone pair in model i, the *p*-type lone pairs are the most basic, they will therefore be involved in binding to the metal. Since they lie at ca. 90° to the C–Hal vector, the C–Hal–M angle is 100–107° not 180° (if the *sp* orbital were chosen) nor 110°, the value of C–P–M in typical PR_3 complexes such as **2** and **5**. This picture also explains why the angles change as they do on descending group 17: the result of the greater contribution of model i to the structure of RI compared to RBr and RCl.

An attempted fluorocarbon analogue

The corresponding fluorocarbon complex $[IrC(cod)(\eta^1\text{-}PPh_2(o\text{-}FC_6H_4)]$ was readily prepared by the method used for the other analogs. The phosphine was nonchelating as shown by the ^{31}P NMR. Unfortunately, treatment with $AgSbF_6$ led to the formation of an uncharacterized mixture of products and not the desired fluoro-bound chelate.

The rhodium analog of 2

In order to verify that halocarbon binding is also possible in the second row analogues, we studied complexes of L^{Br} with $[Rh(cod)Cl]_2$. Analogues of **1** and **2** were prepared by methods similar to the ones used for the Ir species. Once again the ^{31}P NMR suggests that the analog of **1** is nonchelating (δ +28.25 ppm, d, ^1J(P,Rh) 145 Hz), while that of **2** is chelating (δ +59 ppm, d, ^1J(P,Rh) 141 Hz).

Bonding of the halocarbons to the metal

As suggested by the structural data, the halocarbon seems to be acting as a Lewis base via its largely *p*-type lone pairs. In principle, the metal could also be filling the C–Hal σ^* orbital by back donation. That the binding of the halocarbon is encouraged by the electrophilicity of the metal (compare the cases of **1** and **2**),

suggests that the latter is a minor contributor. The largely σ acceptor character of the metal also encourages the binding of 'agostic' C–H bonds and of molecular H_2 in closely related systems [17a]. It may be that a binding site that tends to form one of these structures is a good candidate for binding the other ligands in a nondissociated form. The reason that a σ-acceptor metal may favor nondissociative binding of all three ligands is that depleting the C–X or H–H σ bond weakens, but does not break that bond. A good π-donor metal, on the other hand will tend to occupy the $\sigma^\star$ levels of the ligands and so break the C–X or H–H σ bonds to give dissociative binding (oxidative addition). The factors that will probably favor nondissociative binding of halocarbons are (i) electron acceptor ligands and (ii) the presence of a positive charge. It remains to be seen how far these expectations will be borne out in practice.

Experimental

o-$BrC_6H_4PPh_2$ was purchased from Organometallics Inc. (^{31}P NMR: δ −7.3 ppm), *o*-$ClC_6H_4PPh_2$ was prepared according to Hart [20]. *o*-$FC_6H_4PPh_2$ was a gift of Dr. R.J. Uriarte (General Electric Corp.).

Crystallography

Crystals of [Ir(cod)Cl(*o*-$C_6H_4(X)PPh_2$)] (X = Br (**2**), X = Cl (**6**)) were mounted on a Syntex P3 automated diffractometer. Unit cell dimensions (Table 1) were determined by least squares refinement of the best angular positions for 15 independent reflections ($2\theta > 15°$) during normal alignment procedures using molybdenum radiation (λ 0.71069 Å). Data (7342 points **2**; 7641 points, **6**) were collected at 20 °C using a variable scan rate, a θ–2θ scan mode and a scan width of 1.2° below K_{α_1} and 1.2° above K_{α_2} to a maximum 2θ of 116°. Backgrounds were measured at each side of the scan for a combined time equal to the total scan time. The intensities of three standard reflections were monitored after every 97 reflections and as these intensities showed less than 8% variation, decomposition corrections were not made. Data were corrected for Lorentz, polarization and background, but not absorption effects. 3863 reflections were considered observed. [$I > 3\sigma(I_0)$]. The positional parameters were calculated using normal geometry and an 0.97 Å C–H distance. These hydrogen positional parameters were included but held constant in the final cycle of refinement with isotopic thermal parameters of $U = 0.03$. The final cycle of refinement (Function minimized $\Sigma(|F_0|^2 - |F_c|^2)$ led to a final agreement factor $R = 6.7\%$. ($R = (\Sigma||F_0| - |F_c||/\Sigma|F_0|) \times 100$). Anomalous dispersion corrections were made for Ir, Sb, Cl and P. Unit weights were used throughout.

The same procedure was used for the bromo analogue but 3213 reflections were used and the final R value was a less satisfactory 9.6%, probably due to disorder in the SbF_6 and cod groups. Some disorder was also noted in the chloroarene analogue.

η^2-(η^4-Cyclooctadiene){η^2-halophenyl(diphenylphosphine)}iridium(I) hexafluoroantimonate

Step I. To $[IrCl(cod)]_2$ (300 mg, 0.447 mmole) in CH_2Cl_2 (15 ml) was added the appropriate phosphine (0.984 mmol) and the mixture stirred for 12 h at 25 °C. The volume of the solution was reduced to 5 ml and heptane (20 ml) added to precipitate the yellow solids in 80–85% yield. The three complexes (X = F, Cl and

Table 4

NMR data for the complexes studied.

Compound	^{1}H NMR [a]	^{31}P NMR
[IrCl(cod)(η^1-L^{Br})]	1.65–2.15, c (br), cod-allyl; 3.10, br, 2H, cod-vinyl *trans* to Cl; 5.11 br, 2H, cod-vinyl *trans* to P; 6.95, c, 1H, phenyl; 7.25, c, phenyl	1.19
[IrCl(cod)(η^1 – L^{Cl})]	1.6–2.25, c (br), cod-allyl; 3.07, br, 2H, cod-vinyl; 5.00, br, 2H, cod-vinyl; 6.96–7.2, c, 1H, phenyl; 7.47–7.75, c, phenyl	17.3
[IrCl(cod)(η^1-L^{F})]	1.6–2.3, c (br), cod-allyl; 2.85, br, 2H, cod-vinyl; 5.14, br, 2H, cod-vinyl; 7.0–7.2, c, 1H, phenyl; 7.41–7.75, c, phenyl	–
[RhCl(cod)(η^1-L^{Br})]	1.8–2.3, c (br), cod-allyl; 3.69, br, 2H, cod-vinyl; 5.49, br, 2H, cod-vinyl; 6.9, c, 1H, phenyl; 7.307.8, c, phenyl	28.2 [b]
[Ir(cod)(η^2-L^{Br})]SbF_6	1.68–2.25, c, (br), cod-allyl 3.49, br, 2H, cod-vinyl *trans* to Br; 5.75, br, 2H, cod-vinyl *trans* to P; 7.54, c, phenyl	52.7
[Ir(cod)(η^2-L^{Cl})]SbF_6	1.8–2.3, c (br), cod-allyl; 3.69, br, 2H, cod-vinyl; 5.61, br, 2H, cod-vinyl; 7.45–7.85, c, phenyl	45.9
[Rh(cod)(η^2-L^{Br})]SbF_6	2.1–2.5, c (br), cod-allyl; 3.95, br, 2H, cod-vinyl; 5.79, br, 2H, cod-vinyl; 7.3–7.6, c, phenyl	59.0 [c]
[Ir(cod)(MeCN)(η^1-L^{Br})]SbF_6 [d]	1.7–2.5, c (br), cod-allyl; 4.53, br, 4H, cod-vinyl; 6.80–7.05, c, 1H, phenyl; 7.4–7.65, c, phenyl; 7.9–8.05, c, phenyl	19.9
[Ir(cod)(MeCN)(η^2-L^{Br})]SbF_6	1.82, s, MeCN; 1.7–2.25, c (br), cod-allyl; 3.11, br, 1H, cod-vinyl; 4.10, br, 1H, cod-vinyl; 4.77, br, 1H, cod-vinyl; 4.97, br, 1H, cod-vinyl; 6.8–7.9, c, phenyl	
[IrH_2(cod)(η^2-L^{Br})]SbF_6	–17.6, d, 12.4, Ir-H^a; –12.6, d, 17.7, Ir-H^b; 1.9–2.6, c (br), cod-allyl; 4.198, br, 1H, cod-vinyl; 4.39, br, 1H, cod-vinyl; 5.59, br, 1H, cod-vinyl; 6.00, br, 1H, cod-vinyl; 7.2–8.3, c, phenyl	42.5

Table 4 (continued)

Compound	^{1}H NMR [a]	^{31}P NMR
[IrBr(cod)(PPh_3)]	1.2–2.2, c (br), cod-allyl; 2.94, br, 2H, cod-vinyl *trans* to Br; 5.60, br, 2H, cod-vinyl *trans* to P; 7.0–7.85, c, phenyl	19.4
[IrMe(cod)(η^1-L^{Br})]	0.83, d, 6.2, Ir-Me; 1.7–2.3, c (br), cod-allyl; 3.60, br, 2H, cod-vinyl *trans* to Me; 4.42, br, 2H, cod-vinyl *trans* to P; 6.6–6.75, c, 1H, phenyl; 7.03–7.65, c, phenyl	30.5
[IrMeH$_2$(cod)(η^1-L^{Br})]	−10.55, dd, 33.6 and 15.2, Ir-H *cis* to P; −9.4, dd, 118.2 and 15.2, Ir-H *trans* to P; 0.79, d, 10.7, Ir-Me; 1.2–2.3, c (br), cod-allyl; 2.5–5.7, br, cod-vinyls; 6.54, c, phenyl; 6.9–8.1, c, phenyl	36.2
[IrH(cod)(η^1-L^{Br})] [e]	−8.46, d, 21.1, Ir-H; 3.27 and 4.26, br, cod-vinyl; 7.1–7.6, c, Ar	17.4

[a] All NMR data are reported as chemical shift (ppm), multiplicity (s, singlet; d, doublet; t, triplet; dd, doublet of doublets; br, broad; c, complex), coupling constant (J(PH) and J(HH)) in Hz, integrated intensity, and assignment. All spectra were recorded at 25 °C unless otherwise stated. The ^{31}P NMR of free ligands was: L^{Cl}, δ −13.228; L^{Br}, δ −7.328; PPh_3, δ −7.70 ppm. [b] This ^{31}P resonance appears as a doublet with J(Rh–H) 145 Hz. [c] The ^{31}P resonance appears as a doublet with J(Rh–H) 141 Hz. [d] This complex [19] is in equilibrium with the chelated form at room temperature. [e] ^{1}H NMR measured at −80 °C (193 K).

Br) were isolated by filtration, washed with heptane and dried in vacuo. The rhodium analog of the bromoarene was prepared by an analogous method in 65% yield.

Step II. The bromo- and chloroarene complexes prepared by the route described above (0.838 mmole) were dissolved in CH_2Cl_2 and treated with $AgSbF_6$ (288 mg, 0.838 mmole). The reaction mixture was stirred for 20 min in the dark, filtered through Celite and concentrated to 5 ml. Et_2O (40 ml) was added and the products were precipitated as orange solids in 89–93% yield. Anal. Found: C, 35.51; H, 3.10; Br 8.91. $C_{26}H_{26}BrF_6PSbIr$ calcd.: C, 35.59; H, 2.99; Br, 9.11%. Found: C, 37.47; H, 3.17; Cl, 4.93. $C_{26}H_{26}ClF_6PSbIr$ calcd.: C, 37.49; H, 3.15; Cl, 4.26%. Found C, 39.59; H, 3.47; Br, 9.61. $C_{26}H_{26}BrF_6PSbRh$ calcd.: C, 39.62; H, 3.33; Br, 10.14%. NMR spectra of these and all the species studied are reported in Table 4. The bromoarenerhodium analogue was prepared by the same method in 85% yield.

Reactions of [Ir(cod)(η^2-o-$BrC_6H_4PPh_2$)]SbF_6 2 with H_2. Through a solution of **2** (100 mg, 0.114 mmole) in CH_2Cl_2 (5 ml) at 0 °C was bubbled H_2 (1 atm, ca. 100 ml/min) for 4 min Et_2O (35 ml) was added while maintaining the H_2 atmosphere and a colorless precipitate of the dihydride was formed. This was isolated by filtration, washed with Et_2O (3 × 3 ml) and dried in vacuo for 1 h. It was unstable on heating and therefore was not analysed.

With NaCl: To **2** (50 mg, 0.057 mmol) in acetone-d_6 (0.6 ml) in an NMR tube was added NaCl (33 mg, 0.56 mmol). The ^{1}H NMR spectrum showed complete conversion to [IrCl(cod)(η^1-*o*-$BrC_6H_4PPh_2$)] over 2 h. In CD_2Cl_2, the reaction took 5 h.

With MeCN: To **2** (100 mg, 0.114 mmol) in CH_2Cl_2 (5 ml) was added MeCN (6.0 μl, 0.114 mmol). After 1 h, Et_2O (30 ml) was added to precipitate the product which was recrystallized from CH_2Cl_2/Et_2O (1/6, 35 ml). NMR data showed that the product is **2** even though an NMR spectrum of an exactly similar solution (but in CD_2Cl_2) showed that $[Ir(cod)(MeCN)_x(\eta^1\text{-}o\text{-}BrC_6H_4PPh_2)]^+$ was formed. At $-80\,^\circ C$, however, a 5-coordinate adduct was formed first, as judged by NMR studies (Table 4).

With $LiBEt_3H$: To **2** (50 mg, 0.057 mmole) in dry THF (15 ml) or toluene (10 ml) was added $LiBEt_3H$ (57 μl of a 1 *M* solution in THF, 0.057 mmole), and the mixture was stirred for 10 h at 25 °C. After the addition of EtOH (1.5 μl, 0.029 mmol), the mixture was filtered (Celite) and the resulting orange solution evaporated in vacuo to give an orange solid. ^{1}H and ^{31}P NMR data (Table 4) indicated the formation of [Ir(cod)PPh_3Br], which was also, independently prepared from [IrCl(cod)PPh_3] (56 mg, 0.094 mmole) and LiBr (81 mg, 0.094 mmole) in acetone (10 ml) at room temperature for 60 min. The same product was obtained from **1** (75 mg, 0.11 mole) and $LiBEt_3H$ (110 μl of a 1 *M* solution in THF in THF, 0.11 mole). The free phosphine, L^{Br}, (34 mg, 0.1 mmole) did not react with $LiBEt_3H$ (100 μl of 1 *M* solution in THF) in THF (10 ml) for 10 h at 25 °C.

With sodium formate: **2** (50 mg, 0.057 mmole) and sodium formate (39 mg, 0.057 mmole) were stirred in CH_2Cl_2 at 25 °C for 44 h. The mixture was filtered through Celite and the resulting solution evaporated to 3 ml. Heptane (10 ml) gave [IrBr(cod)(PPh_3)] as an orange solid (40 mg, 80%) which was filtered, washed with heptane (2 × 2 ml) and dried in vacuo. It was identical (NMR, IR) to authentic material prepared as described above.

With MeLi: To **2** (350 mg, 0.4 mmole) in THF (20 ml) at 0 °C was added MeLi (530 μl of 1.5 *M* solution in Et_2O, 0.8 mmole) dropwise. The solution turned from orange to cherry-red and after stirring for 1 h at 0 °C, MeOH (1.8 μl, 0.44 mole) was added to quench any unreacted MeLi. After evaporation in vacuo; benzene (20 ml) was added, the mixture filtered through Celite, the solution evaporated to 3 ml and heptane (10 ml) added to precipitate [Ir(cod)(η^1-L^{Br})Me] (**4**) as an air sensitive red solid. This was filtered, washed (2 × 2 ml heptane, −20 °C) and dried in vacuo. Yield: 186 mg (71%). The same product was formed in similar yield from **1** and LiMe by an analogous procedure. It was too air-unstable for successful microanalysis.

*Reactions of [IrMe(cod)(η^1-L^{Br})] (**4**): With HBF_4.* To **4** (50 mg, 0.067 mmole) in benzene (10 ml) was added $HBF_4 \cdot Et_2O$ (9.8 μl, 0.084 mmol). The solution turned to orange from red and after 3 min an orange solid precipitated. After 15 min this solid was filtered, washed (3 × 3 ml pentane) and dried in vacuo to give **2** in essentially quantitative yield.

With H_2: To **4** (26 mg, 0.04 mmol) in toluene-d_8 (0.5 ml) in an NMR tube was added H_2 by bubbling the gas through the sample for 2 min. The red color was lost and the resulting solution gave the NMR spectrum at −80 °C described in Table 4 and characteristic for *cis*-[Ir(Me)H_2(cod)(η^1-L^{Br})]. Integration of the spectrum showed that the yield of dihydride was 80%. Over 2 h CH_4 was lost and

[IrH(cod)(η^1-L^{Br})] formed. The same monohydride was prepared independently from **1** (28 mg, 0.04 mol) and $LiBEt_3H$ (40 μl of 1 *M* solution in toluene) in toluene-d_8 at $-80\,^\circ C$ in an NMR tube.

Supplementary material available. The full X-ray data for the bromo-complex was deposited with our original communication (ref. 4c) and can be ordered by consulting any current masthead page of 'Organometallics'. The data for the chloro-analog can be obtained from E.M.H. or R.H.C.

Acknowledgement

We thank the Petroleum Research Fund for funding and the Camille and Henry Dreyfus Foundation for a Fellowship (R.H.C.).

References

1 D.N. Lawson, J.A. Osborn and G. Wilkinson, J. Chem. Soc. (A), (1966) 1733.
2 W. Beck and K. Schloter, Z. Naturforsch. B, 33 (1978) 1214; 35 (1980) 985.
3 P.G.H. Troughton and A.C. Skapski, Chem. Comm., (1968) 575.
4 (a) R.H. Crabtree, J.W. Faller, M.F. Mellea and J.M. Quirk, Organometallics, 1 (1982) 1361; (b) M.J. Burk, R.H. Crabtree and B. Segmuller, ibid., submitted; (c) M.J. Burk, R.H. Crabtree and E.M. Holt, ibid., 3 (1984) 638.
5 (a) F. Barcelo, P. Lahuerta, M.A. Ubeda, C. Foces-Foces, F.H. Cano, and M. Martinez-Ripoll, Chem. Comm., 43 (1985); (b) F.A. Cotton and P. Lahuerta, Inorg. Chem., 25 (1986) 3526; (c) H.H. Murray and J.P. Fackler, Chem. Comm., (1985) 1278.
6 R.M. Catala, D. Cruz-Garritz, A. Hills, D.L. Hughes, R.L. Richards, P. Sosa and H. Torrens, Chem. Comm., (1987) 261; R. Uson, J. Fornies, M. Tomas, F.A. Cotton and L.R. Falvello, J. Am. Chem. Soc., 106 (1984) 2482; R.H. Crabtree, E.M. Holt, M. Lavin, and R.J. Kulawiec, Inorg. Chem., submitted.
7 P.E. Garrou, Chem. Revs., 81 (1981) 229.
8 K. Vrieze, H. Volger and A.P. Praat, J. Organomet. Chem., 14 (1968) 185 and 429; R.H. Crabtree and G.E. Morris, ibid., 135 (1977) 395.
9 L. Vaska, Accts. Chem. Res., 1 (1968) 335.
10 R.H. Crabtree, H. Felkin, T. Fillebeen-Khan, and G.E. Morris, J. Organomet. Chem., 168 (1979) 183.
11 R.H. Crabtree, M.F. Mellea, J.M. Mihelcic, and J.M. Quirk, J. Am. Chem. Soc., 104 (1982) 107.
12 R.H. Crabtree, C.P. Parnell and R.J. Uriarte Organometallics, 6 (1987) 696.
13 M.F. Lappert, P.W. Lednor Adv. Organomet. Chem., 14 (1900) 345.
14 J.Y. Saillard and R. Hoffmann J. Am. Chem. Soc., 106 (1984) 2006.
15 G.J. Kubas, C.J. Unkefer, B.I. Swanson, and E. Fukushima, J. Am. Chem. Soc., 108 (1986) 7000.
16 R.H. Morris, J.F. Sawyer, M. Shiralian, J.D. Zubkowski, J. Am. Chem. Soc., 107 (1985) 5581.
17 (a) R.H. Crabtree, M. Lavin and L. Bonneviot, J. Am. Chem. Soc., 108 (1986) 4032; (b) J.W. Suggs, S.D. Cox, R.H. Crabtree and J.M. Quirk Tetrahedron Lett., 22 (1981) 303.
18 (a) J.V. Ortiz, Z. Havlas, and R. Hoffmann, Helv. Chem. Acta, 67 (1984) 1; (b) R.A. Dubois, P.E. Garrou, K.D. Lavin and H.R. Allcock, Organometallics, 3 (1984) 649.
19 A. Skancke, J. Mol. Struct., 42 (1977) 235.
20 F.A. Hart, J. Chem. Soc., (1960) 3324.
21 J.M. Steward (Ed.), The X-ray System-Version of 1980, Technical Report TR446, Computer Center, University of Maryland, College Park, MD.